



Synthesis, Bioactivity and Antimicrobial Studies on Zinc Oxide Incorporated into Nanohydroxyapatite



Adli A. Hanna¹, Lobna A. Khorshed², Ahmed A. El-Beih³, Marwa A. Sherief^{1*}, Amany A. El-Kheshen⁴, Gehan T. El-Bassyouni⁵

¹Inorganic Chemistry Department, National Research Centre, 33 Elbohooth St.(Tahrir) Dokki, P.O.Box:12622, Postal code: 11787, Giza, Egypt.

²Physical Chemistry Department, National Research Centre, 33 Elbohooth St.(Tahrir) Dokki, P.O.Box:12622, Postal code: 11787, Giza, Egypt.

³Chemistry of Natural & Microbial Product Department, National Research Centre, 33 Elbohooth St.(Tahrir) Dokki, P.O.Box:12622, Postal code: 11787, Giza, Egypt.

⁴Glass Research Department, National Research Centre, 33 Elbohooth St.(Tahrir) Dokki, P.O.Box:12622, Postal code: 11787, Giza, Egypt.

⁵Refractories, Ceramics and Building Material Department, National Research Centre, 33 Elbohooth St.(Tahrir) Dokki, P.O.Box:12622, Postal code: 11787, Giza, Egypt.

THIS study reports the influence of zinc oxide (ZnO) on the bioactivity and antimicrobial properties of nanohydroxyapatite. Nanoparticles of hydroxyapatite (HA) were prepared by a sol-gel method. The dried prepared particles were mixed with different percentages of ZnO (25, 50 and 75% wt. %). The produced samples were characterized by fourier transform infrared (FTIR) and X-ray diffraction (XRD), scanning electron microscopy (SEM), transmission electron microscopy (TEM) and energy dispersive X-ray (EDAX) techniques. The results indicate that the pure HA is formed in nanoparticles (<100 nm) and have a hexagonal structure. By adding different percentages of ZnO, the particles exhibit a decrease in their size and improve the crystallinity of the parent HA. Before studying the bioactivity, the prepared samples were immersed in simulated body fluid (SBF) solution for 14 and 45 days. The characterization of the samples after immersion indicates that there is no change in the structure and in the phases, while there are changes in the Ca/P ratio. The bioactivity behavior of the pure HA and their mixed samples toward a gram-positive bacterium (Staphylococcus aureus ATCC 29213), gram-negative bacterium (Escherichia coli ATCC 25922), yeast (Candida albicans NRRL-Y477) and (Aspergillus niger NRC53) fungus signified that the addition of the ZnO increased the resistance of samples against bacteria activity and did not have effects on the fungi and yeast.

Keywords: Synthesis, Hydroxyapatite, Zinc oxide, Characterization, Bioactivity, Antimicrobial

Introduction

One of the medical fields that had been progressed from the development of nanomedicine modules is the orthopedic surgeries [1]. The developing of biomaterial engineering needs to modify the synthetic biomaterials used in this field. Among the synthetic biomaterials, hydroxyapatite (HA) has gained a special attention because it has

excellent chemical, mechanical and structural properties. Moreover, it is nontoxic materials with osteoinductive properties and it has a similar composition and structure of the bone tissue [2,3]. The improvements of the hydroxyapatite go into two directions. The first one is preparing the HA particles in the nano-size scale with high surface area, this improves their stability for restoration

*Corresponding author email: gohamora@yahoo.com

Received 19/5/2019; Accepted 13/6/2019

DOI: 10.21608/ejchem.2019.12988.1812

©2019 National Information and Documentation Center (NIDOC)

of hard tissues such as bone and teeth. On other hand, the HA nanoparticles have an excellent adsorption properties to be used in the removing of toxic materials such as dyes and heavy materials, furthermore it was used as a carrier for drugs [4]. The second improvement of HA particles is carried out by doping or mixing with some other cations in order to enhance the medical and the biological properties of the HA [5]. The chemical composition of HA consists mainly of three active groups, namely: calcium (Ca^{2+}), phosphate (PO_4^{3-}), and hydroxide (OH^-). The presence of such groups leads to form different formula when mixed with other foreign elements through the electrostatic force or substituted with cations such as:

- i) The mono valence cations such as K^+ , Na^+ , the divalent cations such as Mn^{+2} , Ni^{+2} , Cu^{+2} , Co^{+2} , Pb^{+2} , etc.; and the trivalence cations such as Y^{+3} , La^{+3} , Ce^{+3} and A^{+3} can be substituted with Ca^{+2} ions by different ratios.
- ii) The carbonates of As, Si, V, Cr, etc.; can be incorporated with the PO_4^{3-} .
- iii) The hydroxide group of HA can be mixed or substituted with F^- , Cl^- , OH^- and Br^- anions.

However, several works were devoted to explain the effects of the mixing ions on the biological behavior of the parent HA [6-8]. Among the mixing cations, special interest was focused on the zinc (Zn^{+2}), because its incorporation into HA units affects on the biological processes such as enzyme activity, nucleic acid metabolism, mountain of membrane structure and function, as well as biomineralization, and pathological classification [9]. Moreover, teeth have also been found to contain a significant amount of zinc, used as an indicator of environmental explore. In this respect, few researchers found that the incorporation of Zn^{+2} into HA inspires bone formation by activating the osteoblast differentiation and decreasing the osteoclast bone [10,11]. Thus the incorporation of Zn^{+2} ions as ZnO into HA units affects generally the physical, chemical and biological properties of HA.

Therefore, the aim of this work was devoted to prepare both pure HA nanoparticles and its mixing with Zn^{+2} by using a sol-gel method to study the effect of adding Zn^{+2} amounts on the structure and crystallinity of HA units. This work also extends to study the effect of adding Zn^{+2} on the bioactivity of HA [9,12]. The resultant pure HA nanoparticles and ZnO mixed with HA products were characterized by FTIR, XRD and

SEM supplemented with EDAX.

Experimental

Preparation of the samples

Nanohydroxyapatite (HA) powders were prepared using a sol-gel method described elsewhere [9]. About 0.55 M of calcium hydroxide $\text{Ca}(\text{OH})_2$ and 0.33 M of diammonium hydrogen phosphate $(\text{NH}_4)_2\text{HPO}_4$ as sources for calcium and phosphorous respectively. Then, $\text{Ca}(\text{OH})_2$ and $(\text{NH}_4)_2\text{HPO}_4$ were separately dissolved in 500 ml deionized water to obtain a stoichiometric molar ratio of 1.67. The pH of the aqueous solution was maintained at 11 by adding ammonium hydroxide solution NH_4OH [9,13-18]. A gelatinous white precipitate was produced by a dropwise addition of $(\text{NH}_4)_2\text{HPO}_4$ solution to $\text{Ca}(\text{OH})_2$ solution under vigorous stirring at 333 K for one hour. The resultant precipitate was aged for 24 h at room temperature and separated followed by washing with deionized water and then dried in hot air oven at 423 K for 10 h.

HA nanoparticles with varying amounts of ZnO were synthesized using mixed aqueous solutions of prepared pure HA nanoparticles powder and ZnO. The percentage weight of ZnO was varied in the range of: 25, 50 and 75 wt.%. The mixture solutions of HA and ZnO were stirred for one hour. The obtained suspensions were filtered and dried in a hot air oven at 373 K for 5 h.

Characterization of the samples

The prepared dried samples were characterized via different techniques to study the formed phases and their morphologies as follows:

Fourier transform infrared spectroscopy

Fourier transform infrared absorption spectra (FTIR) of the prepared samples were performed by the KBr disc technique using a Fourier transformer infrared spectrometer (Nexus 670 FTIR, USA) in the range 400 to 4000 cm^{-1} .

X-Ray diffraction

X-ray diffraction (XRD) was carried out by using Bruker D8 advance diffractometer (Germany) at $\text{CuK}\alpha$ radiation. Intensity data were collected over the range of 2θ from 10-80°.

Scanning Electron Microscopy (SEM) and Energy Dispersive X-ray (EDAX) Analysis

To give an indication on the surface morphology of samples, SEM coupled with energy-dispersive X-ray spectroscopy (JEOLJXA-840 A, Electron probe micro-analyzer, Japan) was used. Prior to

SEM-EDAX analysis, the samples were coated with gold to overcome the effect of sample charging in the electron beam using a S150A Sputter Coater System, Edwards. There preventative scanning electron micrographs will be selected from several images made of each specimen as a result of much visual observation and selection of each area of the specimen surfaces.

Transmission Electron Microscopy (TEM)

The morphology of produced powder and the particles size were evaluated using a high resolution transmission electron microscope (HR-TEM; JEOL, JEM2100, Electron Microscope, Japan).

Bioactivity tests

To study the bioactivity, 5 g of each powder sample was soaked in 50 ml of Tris-buffered simulated body fluid (SBF) solution, which resembles the human blood plasma at 310K, for 14 and 45 days. The SBF was prepared according to the recommended process by dissolving reagent NaCl, NaHCO₃, KCl, K₂HPO₄·3H₂O, MgCl₂·6H₂O, CaCl₂ and Na₂SO₄ into deionized water as shown in **Table 1**. The solution is buffered to pH 7.4 with tris-(hydroxyl methyl)-amino methane and hydrochloric acid. The immersed samples were taken out after immersion in (SBF). Their characterizations were conducted via FTIR and SEM tools to detect the formation of the hydroxyapatite layer at the surface during the immersion process.

In vitro antimicrobial activity

The ability of the prepared samples to inhibit the growth of the pathogenic microorganisms

was determined against Gram-positive bacterium (*Staphylococcus aureus* ATCC 29213), Gram-negative bacterium (*Escherichia coli* ATCC 25922), yeast (*Candida albicans* NRRL-Y477) and fungus (*Aspergillus niger* NRC53) by the agar diffusion technique.

Bacteria and yeast strains were obtained from the American Type Culture Collection and Northern Regional Research laboratories while the fungal isolates were kindly obtained from the culture collection of the Department of Chemistry of Natural and Microbial Products, National Research Center, Cairo, Egypt. The microorganisms were passaged at least twice times to ensure the purity and the viability. The bacteria were maintained on nutrient agar medium and fungi were maintained on potato dextrose agar (PDA) medium. About 50 mg of the prepared powder samples were applied on the inoculated agar plates and incubated for 24 h at 37°C for bacteria and 72 h at 28°C for fungi. The antimicrobial effect was evaluated by measuring the inhibition zone diameter around the samples in (mm).

Result and Discussion

Investigation of FTIR analysis

The FTIR measurements of the pure and mixed HA with Zn⁺² are shown in **Fig. 1 (a, b, c, and d)**. The FTIR curve of the parent HA (**Fig. 1a**) shows different absorption peaks which specified the formation of HA. It is observed that there are absorption bands at 3436 cm⁻¹ which assigned to OH⁻ stretching vibration and another one appeared at 603.6 cm⁻¹. The final peak is related also to the OH-bending OH-(O-H) in water molecules with HA. On the other hand, two absorption peaks

TABLE 1. The amount of different reagents for preparing the simulated body fluid.

Order	reagent	Amount in gram
1	NaCl	7.996
2	NaHCO ₃	0.350
3	KCl	0.224
4	K ₂ HPO ₄ ·3H ₂ O	0.228
5	MgCl ₂ ·6H ₂ O	0.305
6	1 M HCl	40 ml
7	CaCl ₂	0.278
8	Na ₂ SO ₄	0.071
9	(CH ₂ OH) ₃ CNH ₂	6.057

appeared at 1039 and 566 cm^{-1} corresponded to the phosphate groups attached with the HA. For the HA sample mixed with ZnO, the FTIR spectra **Fig 1(b, c and d)** show a new band at 433 cm^{-1} attributed to the Zn-O stretching mode. As the Zn^{+2} ratios increased the specific band of phosphate group at 1039 cm^{-1} is lowered. This means that the Zn^{+2} cations were incorporated with the HA structure [9,19].

Investigation of XRD patterns

Figure 2 (a, b, c and d) shows the XRD patterns of the pure HA and their corresponding HA mixed with different percentage of ZnO. For the pure HA, different XRD peaks at $2\theta = 26, 28, 32$ and 35°

which specified the monoclinic crystals according to the JCPDS card No (76-0694c). Also, these peaks appeared for the HA mixed with ZnO. The intensities of these peaks increased as the ZnO contents increased. This means that the addition of ZnO improves the crystallinity of the HA. On the other hand, additional peaks appeared at $2\theta = 47, 58, 64$ and 69° upon adding ZnO, as shown in **Fig. 2 (b, c and d)**. The appearance of these peaks affirmed the presence of ZnO according to JCPDS No (89-0510). This finding indicate that the ZnO particles were incorporated into the HA matrix through the electrostatic force. These results are in agreement with the previous works [9,19,20] and as evident by the FTIR results also.

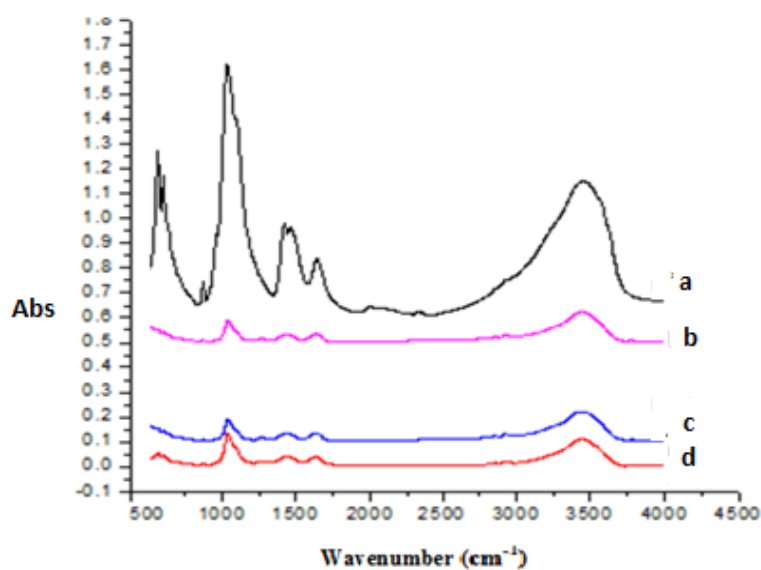


Fig. 1. FTIR spectra of the prepared samples: (a) pure HA, (b) HA with 25%ZnO, (c) HA with 50% ZnO and (d) HA with 75% ZnO.

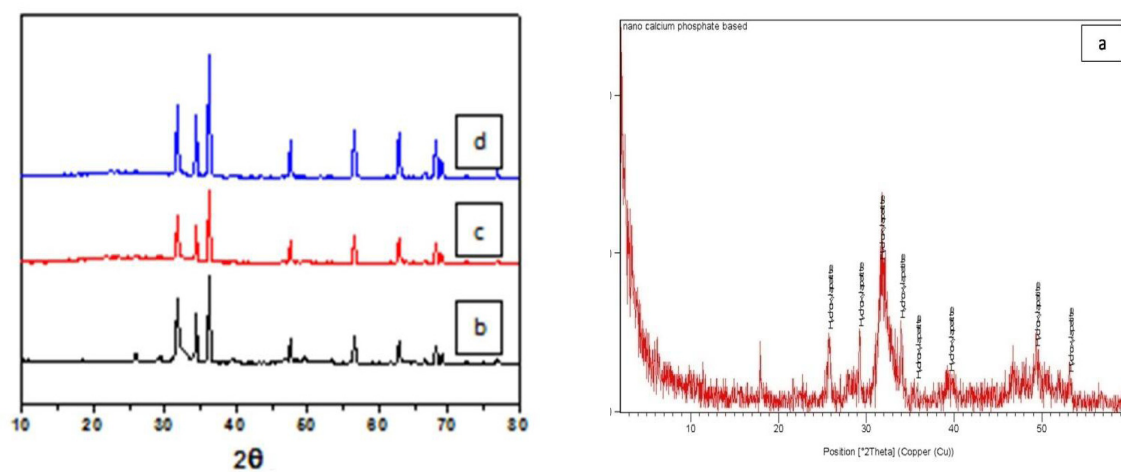


Fig. 2. XRD patterns of samples: (a) pure HA (b) HA with 25%ZnO, (c) HA with 50% ZnO and (d) HA with 75% ZnO.

Investigation of SEM/EDAX analysis

Figure 3 (a, b, c and d) represents the SEM examination of the prepared pure HA and the mixed HA with different amount of ZnO. **Figure 3a** shows the SEM image of the pure HA. It was found to be prepared in nanoparticle sizes (40-100nm) and in the form of hexagonal small rods which are coagulated with each other. **Figure 3b** shows that as ZnO added to HA, the crystals of ZnO are formed in white hard rods-like. It was noticed that the formed HA crystals increased with increasing the percent of ZnO contents as in **Fig.**

3 (c and d). These results are in agreement with the XRD and the FTIR results [9,12]. EDAX analysis confirmed also the presence of Ca, P, O and Zn elements.

TEM analysis

Figure 4 (a, b, c and d) show that the nanoparticles of HA appear in rod-like having nanometer scale dimension, with the selected area diffraction pattern supporting their nanocrystalline nature. When the added ZnO was mixed with HA, there was a significant degree of agglomeration and particles size analysis was not vigorous [21].

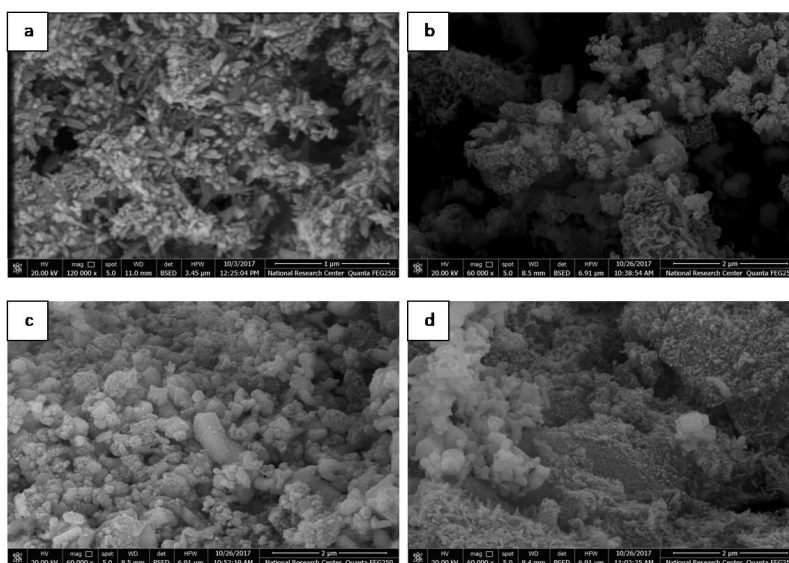


Fig. 3. SEM images of the prepared samples: a) HA pure, b) HA with 25%ZnO, c) HA with 50% ZnO and d) HA with 75% ZnO.

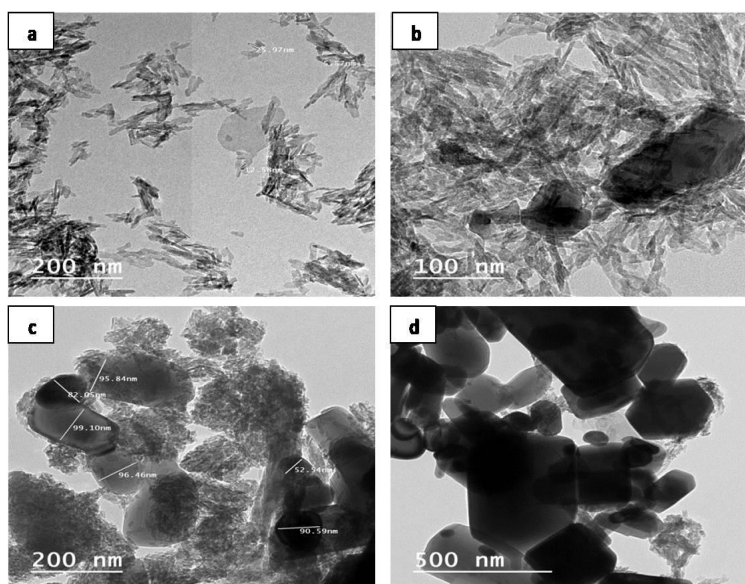


Fig. 4. TEM of the prepared samples: a) HA pure, b) HA with 25%ZnO, c) HA with 50 % ZnO and d) HA with 75% ZnO.

The bioactivity tests

After immersion of pure HA and mixed with ZnO in SBF solution, the structural, crystallinity and morphology of the different samples were examined by using different techniques:-

FTIR spectra after immersion at different soaking periods

After soaking for 14 days, there is no remarkable effect appeared, except the resolution or separation appearance of the band at 1631 cm^{-1} . This may be due to the corrosion and leaching effects of the material in the SBF solution as shown in **Fig. 5A (a-d)**. Where after soaking 45 days, the growth and sharpness of the bands of calcium phosphate at 560 and 620 cm^{-1} appeared and become very clear for mixing HA with 75% of ZnO. This indicates that the immersion of the mixed samples in the SBF exhibits slight effects on the structure of the parent HA and it has more biological effect when mixed with ZnO. This effect was increased as the percentage of ZnO increased as illustrated in **Fig. 5B**.

Scanning electron microscope after immersion at different soaking periods

In nonreactive plastic containers, samples were immersed in SBF solution at different periods of 14 and 45 days.

Figure 6A and B (a, b, c and d) show the SEM images of the pure and the mixed HA

with ZnO after immersion for 14 and 45 days in SBF solutions. For pure HA, it is observed that the particles go in formation of fine regular shape, with decreasing in the particle size, where it becomes $55\text{-}70\text{ nm}$ after immersion for 14 days and decrease to become $32\text{-}54\text{ nm}$ after immersion for 45 days (**Fig. 6A**).

For the samples containing ZnO, the particles exhibit the formation of well defined boundaries and the hexagonal form was predominated. The particles tend to agglomerate as the percentage of ZnO increases from 25 to 75%. This finding indicates that the immersion has a remarkable effect on the shape and the size of the particles and thus inflicts on the structure of the samples.

EDAX analysis provides an elemental analysis of the HA and their mixed samples with ZnO. It is evident that Ca/P ratio was found to be affected by increasing the ZnO content and the time of immersion; they higher than stoichiometric value of 1.67 for HA [i.e. $\text{Ca}_{10}(\text{PO}_4)_6(\text{OH})_2$]. After 14 days, the Ca/P ratio at ZnO_0 , $\text{ZnO}_{25\%}$, $\text{ZnO}_{50\%}$ and $\text{ZnO}_{75\%}$ was 1.86, 2.12, 2.08, and 2.03, respectively. While after immersion for 45 days in SBF, the Ca/P ratio was decreased into 1.54, 1.92, 2.11 and 1.72, respectively. This result revealed a decrease in the Ca^{+2} or an increase in the phosphorus content. This finding concluded that some of the Zn^{+2} was replaced by the Ca^{+2} .

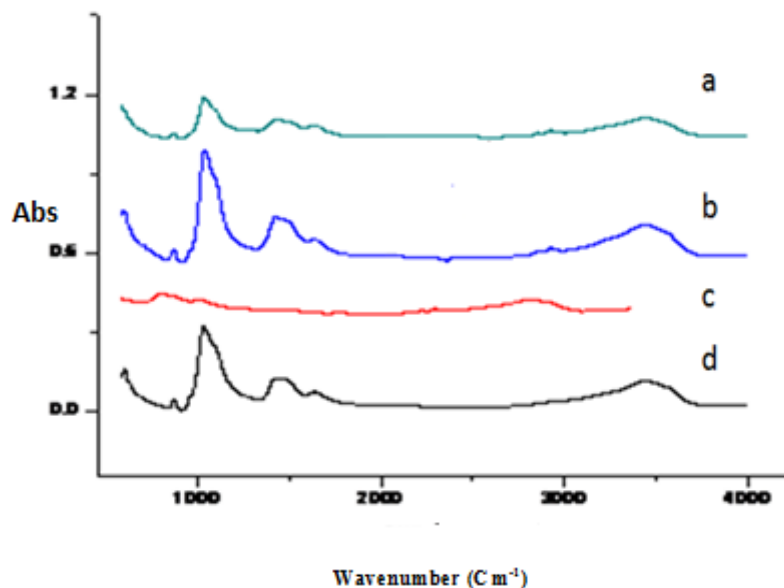


Fig. 5A. FT-IR spectra of prepared samples after soaking in SBF for 14 days: a) HA pure, b) HA with 25% ZnO, c) HA with 50% ZnO and d) HA with 75% ZnO.

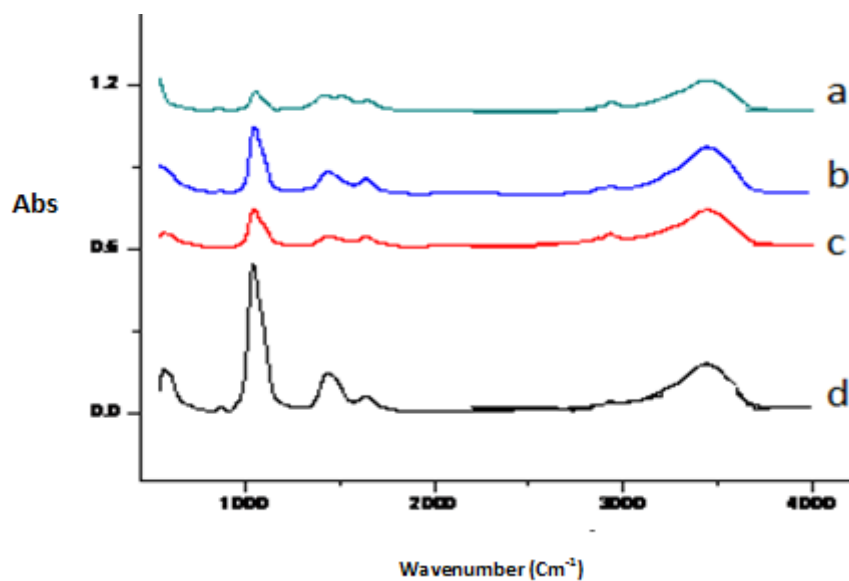


Fig. 5B. FT-IR spectra of prepared samples after soaking in SBF for 45 days: a) HA pure, b) HA with 25% ZnO, c) HA with 50% ZnO and d) HA with 75% ZnO.

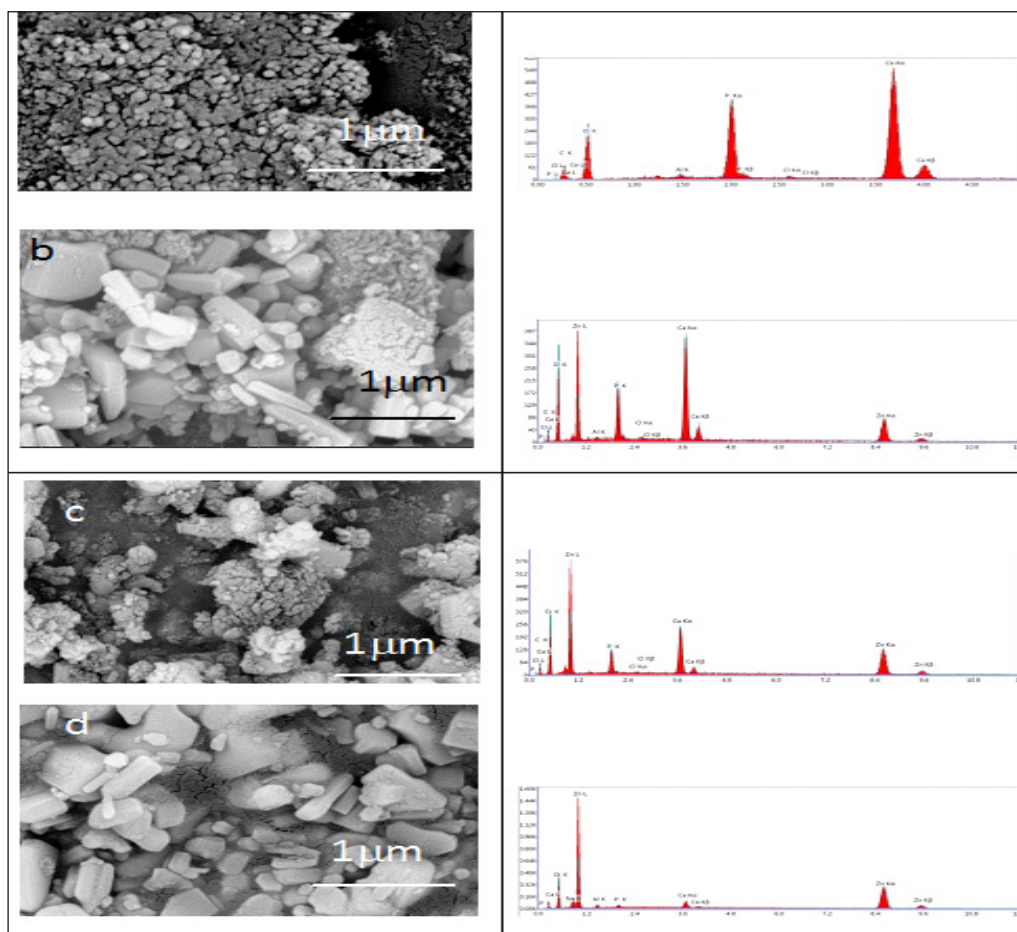


Fig. 6A. SEM and EDAX of prepared samples after soaking in SBF 14 days: a) HA pure, b) HA with 25% ZnO, c) HA with 50% ZnO and d) HA with 75% ZnO.

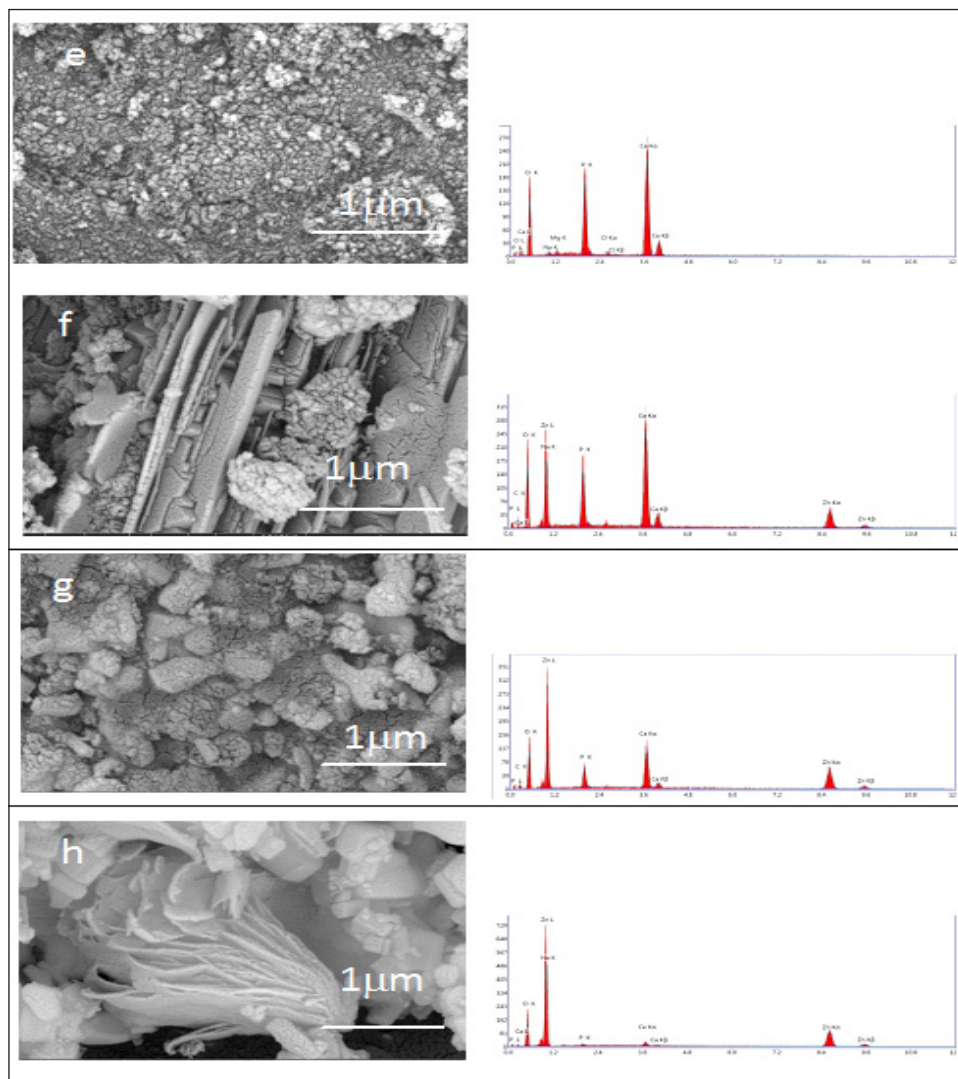


Fig. 6B. SEM and EDAX of prepared samples after soaking in SBF for 45 days: e) HA pure, f) HA with 25% ZnO, g) HA with 50% ZnO and h) HA with 75% ZnO.

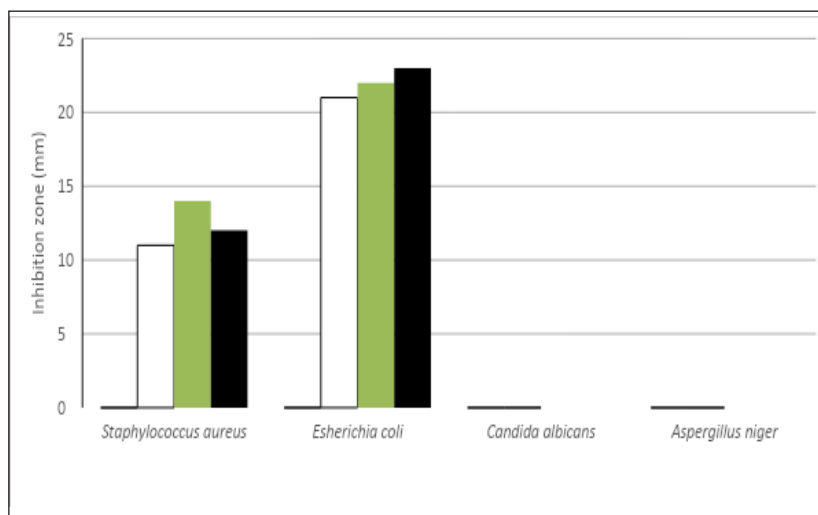
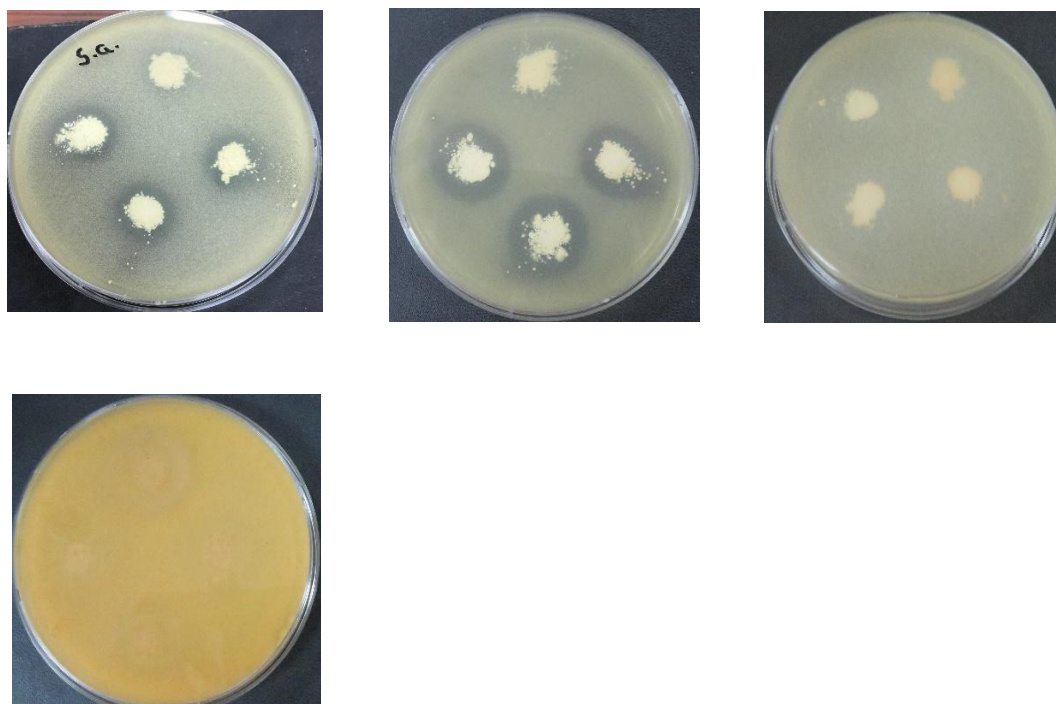
Antimicrobial tests

Antimicrobial results of the samples are shown in **Table 2**. It was revealed that the pure HA didn't show any antimicrobial activity against bacteria or fungi. While, the mixed HA with different weight % of ZnO exhibited strong antibacterial activity with inhibition zones ranging from 11-14 mm for *Staphylococcus aureus* (gram positive) and 21-23 mm for *Escherichia coli* (gram negative, *E. coli*). All tested samples didn't show any activity against fungi and yeast. It has been practically detected that doping of zinc oxide improved the inhibition zones against *Staphylococcus aureus* and *E. coli* pathogens during the antimicrobial study [22, 23] as depicted in **Fig. 7**.

To explain the antimicrobial activity of the zinc ions, there are three main mechanisms [24]. Primary metal ions could bind to the specific groups of the protein chains deactivating them. Next, metal ions can interrelate with microbial membrane and encourage structural and permeability changes. Lastly, metal ions could interact with microbial nucleic acids, inhibiting microbial replication [25]. In **Fig. 8**, results showed that the mixed samples can retain antimicrobial properties and hence the prepared samples can be further used to explore them for future use in clinical applications.

TABLE 2. Inhibition zones on the bacterium and fungus of the prepared samples.

Sample		Inhibition zone (mm)			
		<i>Staphylococcus aureus</i>	<i>Esherichia coli</i>	<i>Candida albicans</i>	<i>Aspergillus niger</i>
HA (ZnO_0)	Series 1	-	-	-	-
$ZnO_{25\%}$	Series 2	11	21	-	-
$ZnO_{50\%}$	Series 3	14	22	-	-
$ZnO_{75\%}$	Series 4	12	23	-	-

**Fig. 7.** Inhibition zone on bacterium and fungus of prepared samples: 1) HA pure, 2) HA with 25% ZnO, 3) HA with 50% ZnO and 4) HA with 75% ZnO.**Fig. 8.** Antibacterial activity of prepared samples against bacterium and fungi: 1) HA pure, 2) HA with 25% ZnO, 3) HA with 50% ZnO and 4) HA with 75% ZnO.

Conclusions

Pure and mixed HA nanoparticles with ZnO samples were prepared via a sol-gel method. The obtained XRD results showed the increase in the crystallite size of HA after mixing with ZnO in the nanoscale. The ZnO incorporation modified the morphology of HA in rod like structure. The analyses of the obtained results show that there is no change in the structure and the phases of the produced HA or HA mixed with different amounts of ZnO, while the crystallinity of HA was improved by increasing the percentages of ZnO. By immersing the pure and the mixed samples in SBF solution, there are slight changes in the FTIR results and increase in the Ca/P ratio which means that P was released in the SBF solution and Ca^{+2} was replaced by some Zn^{+2} . The bioactivity tests show that the adding of ZnO to the HA improves the bioactivity behavior.

References

1. Popa, CL, Deniaud, A, Michaud-Soret, I., Guégan, R, Motelica-Heino, M and Predoi, D., Structural and Biological Assessment of Zinc Doped Hydroxyapatite Nanoparticles. Hindawi Publishing Corporation. *Journal of Nanomaterials*. **2016**, 1-10 (2016).
2. Kolmas, J, Krukowski, S, Laskus, A and Jurkitewicz, M., Synthetic hydroxyapatite in pharmaceutical applications. *Ceramics International* **42**, 2472-2487 (2016).
3. Prekajski Đorđević, M., Maletaškić, J., Stanković, N., Babić, B., Yoshida, K., Yano, T. and Matović, B., In-situ immobilization of Sr radioactive isotope using nanocrystalline hydroxyapatite. *Ceram. Inter.* **44**(2), 1771-1777(2018).
4. Shepherd, JH., Shepherd, DV. and Best, SM., Substituted hydroxyapatites for bone repair. *Journal of Materials Science: Materials in Medicine*. **23**(10), 2335-2347 (2012).
5. Guo, DG., Wang, AH., Han, Y. and Xu, KW., Characterization, physico-chemical properties and biocompatibility of La-incorporated apatites. *Acta Biomaterialia*, **5**(9), 3512-3523 (2009).
6. Mestres, G., Le, Van, C. and Ginebra, MP., Silicon-Stabilized α - tricalcium phosphate and its use in a calcium phosphate cement: characterization and cell response. *Acta Biomaterialia*, **8**(3), 1169-1179 (2012).
7. Ito, A. and Otsuka, M., Zinc-containing tricalcium phosphate and related materials for promoting bone formation. *Curr. Appl. Phys.* **5**, 402-6 (2005).
8. Legeros, RZ., Calcium phosphate-based materials containing zinc, Magnesium, Fluoride and Carbonate. US Patent 7, 419, 680, September 2 (2008).
9. Deepa, C., Begum, AN., and Aravindan, S., Preparation and antimicrobial observations of zinc doped nano-hydroxyapatite, *Nanosystems: Physics, Chemistry and Mathematics*, **4**(3), 370-377 (2013).
10. Uysal, I., Severcan, F. and Evis, Z., Characterization by Fourier transform infrared spectroscopy of hydroxyapatite co-doped with zinc and fluoride. *Ceramics International* **39**, 7727-7733 (2013).
11. Bandyopadhyay, A, Withey, EA., Moore, J. and Bose, S., Influence of ZnO doping in calcium phosphate ceramics. *Mater. Sci. Eng. C*, **27**, 14-17 (2007).
12. Bhattacharjee, P., Begam, H., Chanda, A. and Nandi, SK., Animal trial on zinc doped hydroxyapatite: Acase study. *J. of Asian Cerm. Soci.* **2**, 44-51 (2014).
13. Hann, A. A., Sherief, M. A., Aboelenin, R. M.M., and Mousa, S. M.A., preparation and characterizations of barium hydroxyapatite as ion exchanger. *Canadian Journal of Pure & Applied Science*, **4**(1), 1087-1093 (2010).
14. Hamdy, T. M., Saniour, S. H., Sherief, M. A., and Zaki, D. Y., Effect of incorporation of 20 wt% Amorphous Nano-hydroxyapatite Fillers in Poly methyl methacrylate Composite on the Compressive Strength. *J. of Pharma., Bio. and Chem. Sci. (RJPBCS)*, **6**(3), 1136-1141 (2015).
15. Hassan, S. N., Moharam, L. M., Sherief, M.A., Zaazou, M. H., and Mokhtar, N. Ibrahim Effect of Two Different Remineralizing Agents on the Surface Roughness of Bleached Enamel *J. of Pharma., Bio. and Chem. Sci. (RJPBCS)*, **7**(3), 149-157 (2015).
16. Hanna, A. A., Mousa, S. M.A., Sherief, M.A., and Elkomy, J. M., Synthesis and characterization of nano-sized hydroxyapatite and doped with some rare earth elements from phosphogypsum waste, *International Journal of Chem Tech Research*, **9**(6), 514-523 (2016).
17. Moharam, L. M., Sherief, M. A., and Nagi, S. M., Mechanical properties of resin composite reinforced with synthesized nano-structured

- hydroxyapatite. *International Journal of Chem. Tech. Research*, **9**(7), 634-644 (2016).
18. El Assal, D.W., Saafan, A.M., Moustafa, D.H., Al-Sayed, M.A., The effect of combining laser and nanohydroxy-apatite on the surface properties of enamel with initial defects. *J Clin Exp Dent*. **10**(5), 425-30 (2018).
 19. Zhang, W., Xu, X., Chai, Y. and Wang, Y., Synthesis and characterization of Zn²⁺ and SeO₃-2Co-substituted nano-hydroxyapatite. *Advanced Powder Technology* **27**, 1857-1861 (2016).
 20. Abdul Wahid, MF., Mardziah, CM., Hyie, KM. and Roselina, NRN., Synthesis and characterization of zinc doped hydroxyapatite for bone substituted applications. *Applied Mechanics and Materials*, **660**, 942-946 (2014).
 21. Kumar, GS, Thamizhavel, A., Yokogawa, Y., Kalkura SN and GiriyaEK. Synthesis, characterization and in vitro studies of zinc and carbonate co-substituted nano-hydroxyapatite for biomedical applications. *Mater. Chem. Phys*. **134** (2-3), 1127-1135 (2012).
 22. Thwala, M., Musee, N., Sikhwivhilu, L and Wepener, V., The oxidative toxicity of Ag and ZnO nanoparticles towards the aquatic plant *Spirodelapunctata* and the role of testing media parameters. *Environ. Sci. Process. Impacts* **15**(10), 1830-1843 (2013).
 23. Bhumi, G. and Savithamma, N., Biological synthesis of zinc oxide nanoparticles from *Catharanthus roseus* Linn G. Don leaf extract and validation for antibacterial activity. *Int. J. Drug Dev. Res.* **6**(1), 208-214 (2014).
 24. Marques, CF, Olhero, S, Abrantes, JCC, Marote, A, Ferreira, S, Vieira, SI and Ferreira JMF., Biocompatibility and antimicrobial activity of biphasic calcium phosphate powders doped with metal ions for regenerative medicine. *Ceramics International* **43**, 15719-15728 (2017).
 25. Phan, TN, Bucker, T, Sheng, J, Baldeck, JD and Marquis, RE., Physiologic actions of zinc related to inhibition of acid and alkali production by oral streptococci in suspensions and bio-films. *Oral Microbiol. Immun.* **19**, 31-38 (2004).

تحضير ودراسة الخصائص الحيوية والميكروبية للهيدروكسي أباتيت النانومتري المطعم بأكسيد الزنك

عدي عبد الله حنا¹، لبنى عبدالعزيز فؤاد خورشيد²، احمد عاطف البيه³، مروه عادل السيد حامد⁴، اماتي عبد الحليم الخشن⁵، جيهان التابعي البسيوني⁵

¹قسم الكيمياء الغير عضويه - المركز القومي للبحوث - القاهرة - مصر.

²قسم الكيمياء الفيزيائية - المركز القومي للبحوث - القاهرة - مصر.

³قسم المنتجات الطبيعية والميكروبيولوجيه - المركز القومي للبحوث - القاهرة - مصر.

⁴قسم بحوث الزجاج - المركز القومي للبحوث - القاهرة - مصر.

⁵قسم الحرارية والسيراميك ومواد البناء - المركز القومي للبحوث - القاهرة - مصر.

توضح هذه الدراسة تأثير اضافة أكسيد الزنك بنسب معينه على الخصائص الحيوية و الميكروبية للهيدروكسي أباتيت النانومتري. حيث أنه تم تحضير الهيدروكسي أباتيت بحيث أن تكون جزيئاته في حجم النانومتر وذلك باستخدام طريقة السول - جل. وبعد ذلك تم خلط العينات المحضرة بنسب مختلفه من أكسيد الزنك كالاتي: 25 و 50 و 75 بالنسبه الوزنيه المئوية. وقد خضعت العينات المحضرة من الهيدروكسي أباتيت منفردا وكذلك بعد اضافة أكسيد الزنك له للدراسة والتوصيف باستخدام:- طيف الأشعة تحت الحمراء.- حيود الأشعة السينيه.- الميكروسكوب الالكتروني الماسح المتصل بوحدة التحليل الكيمياء للعينات(EDAX).- الميكروسكوب الالكتروني النافذ.- الدراسة الميكروبيه باستخدام البكتيريا الموجبه والسالبه وكذلك الخميره والفطريات. وقد أثبتت النتائج أن الهيدروكسي أباتيت المحضر بدون اضافة أكسيد الزنك بالفعل في حجم النانومتر (أقل من 100 نانومتر) و تركيبها البللوري سداسي الشكل. وبعد اضافة النسب المختلفه من أكسيد الزنك وجدنا أن حجم الجزيئات أصبح أقل و أيضا حدث زياده في تكوين الأطوار وكثافتها. ويغمر العينات المحضرة في محلول مشابه لبلازما الدم (SBF) لمدة 14 و 45 يوما اتضح أنه لم يحدث أي تغيير في التركيب البللوري و الأطوار المختلفه للعينات و لكن ماحدث هو تغيير في نسبة الكالسيوم الى الفوسفور مما يدل على امكانية استخدام هذا النوع من الهيدروكسي أباتيت المطعم بأكسيد الزنك كماده لها خصائص بيولوجيه وقابله لتكوين طبقة من العظم فوقها عند زرعها في جسم الانسان أو الحيوان. و بالنسبه لدراسة الخصائص الميكروبيه لهذه العينات. فقد تمت باستخدام أنواع من البكتيريا الموجبه (*Staphylococcus aureus* ATCC 29213) والسالبه (*Escherichia coli* ATCC (25922) وكذلك الخميره (*Candida albicans* NRRL-Y477) والفطريات (*Aspergillus niger* NRC53 fungus) وقد أثبتت النتائج المختلفه أن اضافة أكسيد الزنك للهيدروكسي أباتيت أدى الى زياده مقاومة هذه العينات للبكتيريا بنوعها الموجب والسالب ولا يوجد لها أي تأثير على الخميره والفطريات مما يجعلها صالحه لاستخدام كماد بيولوجيه تقاوم البكتيريا .